

Self-Assembled Monolayers of Dioctyl Diselenides on Au(111)

Jungseok Choi, Yoon Jung Lee, Hungu Kang, Jin Wook Han,* and Jaegun Noh*

Department of Chemistry, Hanyang University, Seoul 133-791, Korea. *E-mail: jwhan@hanyang.ac.kr, jgnoh@hanyang.ac.kr

Received March 18, 2008

The surface structure, electrochemical behavior, and wetting property of self-assembled monolayers (SAMs) formed by dioctyl diselenide (DODSe) on Au(111) were investigated by scanning tunneling microscopy (STM), cyclic voltammetry (CV), and contact angle measurements. In contrast to the formation of well-ordered SAMs by octanethiol on Au(111), the SAMs formed by DODSe have a disordered phase and many unusual vacancy islands (VIs). In addition, the formation of DODSe SAMs is largely influenced by the solution concentration used. DODSe SAMs formed in 5 μM and 50 μM solutions have two mixed domains consisting of missing-row ordered phases and disordered phases, while DODSe SAMs formed in 1 mM and 5 mM solutions have only disordered phases with an abnormally high VI fraction of 22-24%. We also found that the wetting property and electrochemical behavior of DODSe SAMs on Au(111) are markedly influenced by the formation of ordered SAMs and the density of VIs.

Key Words : Octanethiol, Dioctyl diselenide, Self-assembled monolayers, Scanning tunneling microscopy, Cyclic voltammetry

Introduction

Self-assembled monolayers (SAMs) provide a very simple method for tailoring surface properties such as wetting, adhesion, corrosion, and lubrication as well as for the fabrication of building block layers. Such layers are applicable to various nanoscale applications such as chemical sensors, electronic devices, and nanolithography.¹⁻¹⁰ To date, SAMs composed of alkanethiols with a sulfur headgroup on gold have been thoroughly studied by means of various surface analyses.^{1-5,10} Due to many efforts, the various fundamental aspects of alkanethiol SAMs, such as the self-assembly mechanism, packing structure, interface dynamics, and thermal and long-term stability, have been clearly revealed.^{1-5,10} It is generally understood that the packing structure and degree of order of SAMs are determined by a complex interplay of sulfur headgroup-gold substrate and intermolecular interactions.

In contrast to many reports regarding thiol SAMs with a sulfur headgroup on gold, there have been only a few reports concerning the molecular features of selenolate SAMs with a selenium headgroup on gold.¹¹⁻¹⁶ The first report by X-ray diffraction measurements suggested that docosaneselenols on gold form ordered SAMs with a ($\sqrt{3} \times \sqrt{3}$) R30° structure.¹¹ Nakano *et al.*¹² reported that the adsorption of decaneselenols on gold surfaces leads to stable SAMs. A scanning tunneling microscopy (STM) study by Dishner *et al.*¹³ revealed that benzeneselenols (BSe) can form well-ordered SAMs with a low molecular density that can be described as a ($3\sqrt{3} \times 2\sqrt{3}$) R30° structure. Surface-enhanced Raman spectroscopy (SERS) by Huang *et al.*¹⁴ demonstrated that the Se-Se bond of diphenyl diselenide (DPDSe) is cleaved to form benzeneselenolates upon adsorption, which is similar to the case of benzenethiolate SAM formation *via* S-S bond cleavage of the diphenyl disulfide.

Similar SERS results were obtained from dialkyl diselenides on gold during self-assembly.¹⁵ Interestingly, a large difference in competitive adsorption of aromatic thiols and seleniums was observed on gold and silver surfaces: the adsorption of DPDSe is more favorable than that of diphenyl disulfide on gold,¹⁴ whereas the opposite adsorption takes place on silver for BSe and benzenethiol.¹⁶

The main purpose of this study is to understand the surface structure and properties of SAMs formed by dioctyl diselenide (DODSe, $\text{CH}_3(\text{CH}_2)_7\text{Se-Se}(\text{CH}_2)_7\text{CH}_3$) on gold. The SAMs were characterized using STM, cyclic voltammetry (CV), and contact angle measurements. We report the first STM results showing phase changes of DODSe SAMs depending on solution concentration, implying that the selection of a suitable solution concentration is one of the most important factors for controlling the two-dimensional SAM structure of dialkyl diselenides. In addition, we demonstrated that the wetting property of DODSe SAMs is strongly related to the formation of ordered SAMs and vacancy islands, which is evidenced by the STM results.

Experimental Section

DODSe was conveniently synthesized by refluxing Na_2Se_2 with $\text{C}_8\text{H}_{17}\text{Br}$ in methanol for 3 h.¹⁷ The product was purified by chromatography on SiO_2 using hexane as an eluent and confirmed by NMR analysis. Octanethiol (OT, $\text{CH}_3(\text{CH}_2)_7\text{SH}$) was purchased from Aldrich. Au(111) substrates were prepared by vacuum deposition onto freshly cleaved mica sheets as described previously.⁵ The SAMs were formed by immersing the Au(111) substrates into freshly prepared 1 mM ethanol solutions of OT and DODSe for one day at room temperature. To investigate the surface structures of DODSe SAMs formed in different solution concentrations, the SAMs were also prepared after immersion for 30 min at

room temperature in 5 μM , 50 μM , 1 mM, and 5 mM solutions. The SAM samples were rinsed thoroughly with ethanol in order to remove physisorbed materials of the surface and blown dry with nitrogen.

STM was carried out using a NanoScope E instrument (Veeco, Santa Barbara, CA) and a commercially available Pt/Ir tip (80:20). All STM images were taken under ambient conditions using the constant current mode. Bias voltages between 250 and 650 mV and tunneling currents between 300 to 550 pA were applied to the tip and samples. CV was performed in a 1-mM $\text{Fe}(\text{CN})_6$ solution with 1 M KCl as the supporting electrolyte. The cyclic voltammograms were carried out in the potential range of -0.5 to $+0.9$ V at room temperature and a scan rate 50 mV/s. The gold substrate with the SAMs monolayer was brought into contact with the electrolyte under the potential control. Contact angle (CA) measurements were performed using an automatic contact angle measuring system (model: Easydrop DSA20S, KRÜSS, Germany). Water contact angles were measured at RT on the SAM samples using the sessile drop method and are an average of CAs obtained from five different sample surfaces.

Results and Discussion

The STM images in Figure 1 show noticeable structural differences between OT and DODSe SAMs on Au(111) prepared after the immersion of gold substrates in 1 mM ethanol solutions of OT and DODSe at room temperature for one day. The STM image in Figure 1a shows typical surface structures of OT SAMs such as a $c(4 \times 2)$ domain structure with a high structural degree of order, clear domain boundaries, and vacancy islands (VIs) with a monatomic step height of 0.24 nm (dark hole), as observed from various alkanethiol SAMs.^{3-5,10} VIs with a round or triangle shape were often observed from alkanethiol SAMs. The surface structures of DODSe SAMs on Au(111), as shown in Figure 1b, are markedly different from those of OT SAMs, even though both molecules have an identical octyl alkyl chain. It was found that DODSe molecules form liquid-like SAMs with the disordered phase containing unclear domain bound-

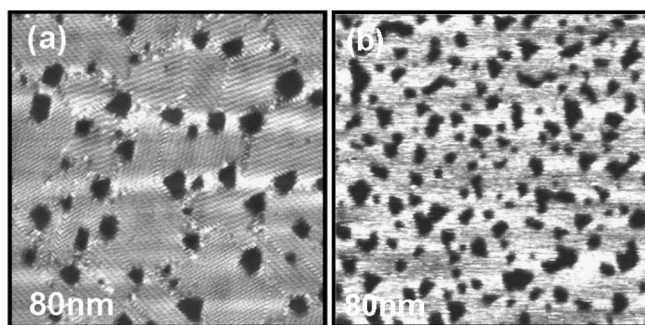


Figure 1. (a) STM images showing surface structures of (a) OT and (b) DODSe SAMs on Au(111) formed one day after immersion of the gold substrates in a 1 mM ethanol solution at room temperature for one day. All scan sizes were 80 nm \times 80 nm. Imaging conditions were (a) $I_b = 0.46$ V, $I_t = 0.36$ nA and (b) $I_b = 0.48$ V, $I_t = 0.38$ nA, respectively.

aries. The obtained STM result is not consistent with the previous results showing the ordered structures of selenium SAMs.¹⁸⁻²⁰ However, it is hard to directly compare our results with other results because target materials and experimental condition (concentration, immersion time and solvent) for SAM preparation are quite different each other. On the other hand, compared with alkanethiol SAMs, DODSe SAMs have irregular-shaped VIs with a high VI density. The ratio of the VI area to the total surface area for DODSe SAMs was measured to be approximately 20-22%, which is markedly larger than the 8-12% observed for OT SAMs. Competitive adsorption experiments monitored by SERS measurements suggested that the selenium-gold bond was stronger than the sulfur-gold bond.¹⁴ Our STM results obtained here are strong nanometer-scale evidence for the formation of a strong chemical bond between the selenium and gold surface, resulting in the effective removal of gold atoms from the first gold layer during the adsorption of DODSe molecules. We also clearly demonstrated that although selenium has the same electron configuration as sulfur, a small difference in interactions between the head-group and gold markedly affects the formation of SAMs and the two-dimensional SAM structure.

To understand the electrochemical behavior of DODSe SAMs on Au(111), we examined that of OT SAMs. Figure 2 shows cyclic voltammograms of (a) bare Au electrode, (b) OT SAMs-, and (c) DODSe SAMs-modified Au electrode in 1 mM $\text{K}_4[\text{Fe}(\text{CN})_6]$ and 1 mM KNO_3 . The peak currents (I_p) for the bare Au electrode and Au electrodes modified with OT and DODSe SAMs were measured to be 507.6, 58.7, and 197.5 $\mu\text{A}/\text{cm}^2$, respectively. Compared with the bare Au electrode, electrodes modified with OT and DODSe SAMs demonstrated noticeably reduced currents, especially in the case of OT SAMs, indicating that SAMs on the Au electrode efficiently blocked the electrode reaction of ferrocyanide. The higher peak current of DODSe SAMs compared with OT SAMs is due to a poor structural order with a higher

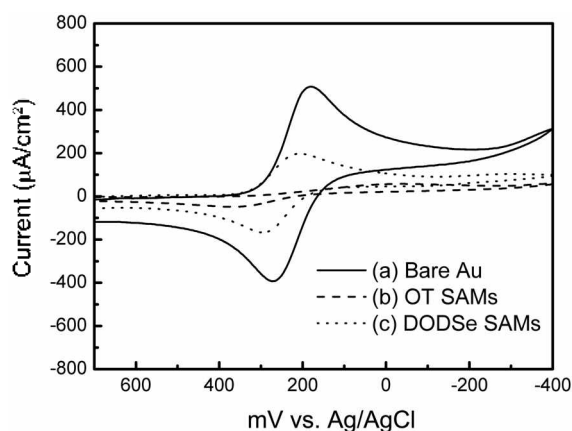


Figure 2. Cyclic voltammograms of (a) bare Au(111) electrode, (b) OT SAMs-, and (c) DODSe SAMs-modified Au(111) electrodes in 1 mM $\text{K}_4[\text{Fe}(\text{CN})_6]$ and 1 mM KNO_3 . The scan rate was 50 mV/s. Note that OT and DODSe SAMs on Au(111) electrode were formed in a 1 mM ethanol solution for one day at room temperature.

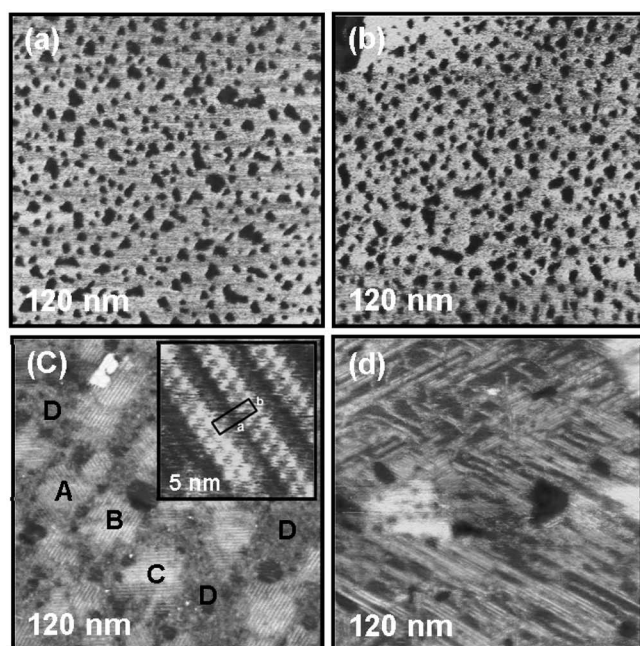


Figure 3. STM images showing surface structures of DODSe SAMs on Au(111) formed after a 30-min immersion of the gold substrates in (a) 5 mM, (b) 1 mM, (c) 50 μM , and (d) 5 μM solutions at room temperature. All imaging conditions were $V_b = 0.46$ V and $I_t = 0.36$ nA. The inset in Figure 3b shows a 5 nm \times 5 nm high-resolution STM image demonstrating DODSe SAMs with a high degree of structural order in the well-ordered domains.

density of VIs, as revealed by STM. This result is in good agreement with the previous result that organic SAMs containing many defects show a higher peak current than SAMs with fewer surface defects in electrochemical measurements.²²

STM images of Figure 3 show surface structures of DODSe SAMs on Au(111) formed after a 30-min immersion of the gold substrates as a function of solution concentration. The surface structures of the SAMs prepared in 5 mM solution, as shown in Figure 3a, are quite similar to those of the SAMs prepared in 1 mM solution (Figure 3b). It is generally considered that a 1 mM solution concentration for the fabrication of alkanethiol SAMs on gold is a typical experimental condition for obtaining fully covered SAMs, which can be formed in a few minutes.^{3,5,10,21} Even though we used concentration greater than the typical condition to expedite the molecular self-assembly of DODSe molecules, we did not observe any ordered structures or structural changes. Contrary to the formation of well-ordered SAMs by thiols in the mM solutions, dialkyl diselenides do not form ordered monolayers under this condition. We then used more dilute (mM) solutions, in which we found that DODSe molecules can form partially ordered domains containing disordered phases, as shown in Figures 3c and d. The STM image of Figure 3c was obtained from DODSe SAMs on Au(111) formed after a 30-min immersion in a 50 μM solution. STM imaging clearly revealed that DODSe SAMs are composed of ordered domains with three-directional domain orientations (regions A, B, and C) and disordered phases (region D). The

observation of three domain orientations indicates that the growth of DODSe SAMs is strongly influenced by the structure of the Au(111) substrate having three-fold gold symmetry. The inset shows the molecularly resolved STM image of ordered domains having missing row phases containing paired molecular rows. The distance (a) between the paired rows is 1.57 nm and the distance (b) between molecules in a row is 0.5 nm. The missing row phase can be considered an incomplete SAM phase that often appears before the formation of closely packed SAMs.²¹ On the other hand, these ordered domains ranging in size from 10 to 25 nm are mainly surrounded by disordered phases (D) and VIs. Considering these STM results, the observed phases in Figure 3c are regarded as an intermediate phase of DODSe SAMs. The STM image of Figure 3d was observed from DODSe SAMs on Au(111) formed after a 3-min immersion in a 5 μM solution. In this diluted solution, DODSe molecules form SAMs that have ordered molecular rows without any clear domain formation and disordered phases, as shown in Figure 3d. In addition, the disordered phases are mainly observed from the internal ordered domains. From these results, we suggest that the formation of defect-free ordered domains is much more energetically favorable than that of ordered domains containing disordered phases, which is driven by an optimization of intermolecular interactions between alkyl chains. It was reported that alkanethiols form closely packed SAMs on gold within 10 min irrespective of the solution concentration from μM to mM scale.²³ Contrary to this, however, we found that DODSe molecules do not form closely packed SAMs in 5 μM or 50 μM solutions, as shown in Figures 3c and d. This result implies that the DODSe molecules having the selenium headgroups require more time to obtain closely packed SAMs.

Figure 4 shows the CAs measured from DODSe SAMs on Au(111) formed after a 30-min immersion of the gold substrates at room temperature as a function of solution concentration. The CAs from the DODSe SAMs formed in 5 μM and 50 μM solutions were measured to be 101° and 98°,

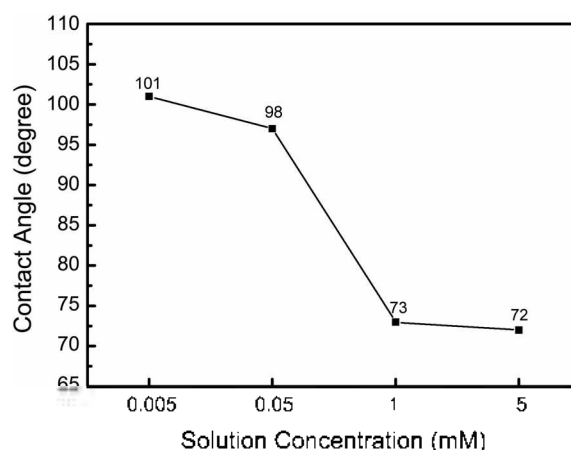


Figure 4. Water static contact angles measured from DODSe SAMs on Au(111) formed after a 30-min immersion of the gold substrates at room temperature as a function of solution concentration.

respectively. These relatively high CAs imply the formation of a hydrophobic surface originating from the presence of a methyl group at the outer SAM surface due to partially ordered phases, as revealed by STM study. On the other hand, the CAs obtained from DODSe SAMs formed in 1 mM and 5 mM solutions were measured to be 73° and 72°, respectively. These CAs are nearly identical, and are relatively smaller than those observed in the low solution concentration. STM imaging clearly revealed that DODSe SAMs have nearly identical structures showing the disordered phase containing an abnormally high number of VIs, which is the main reason for the lower CA values.²²

Conclusion

The surface properties of DODSe SAMs on Au(111) were examined by means of STM, CV, and CA measurements and compared with those of OT SAMs. Even though selenium and sulfur belong to the VIA group of the periodic table, we observed that both SAMs have markedly different surface characteristics in the formation of ordered domains and VIs. Contrary to alkanethiol SAMs, the formation of DODSe SAMs is largely influenced by the solution concentration used. DODSe SAMs formed in 5 μ M and 50 μ M solutions have two mixed domains consisting of missing-row ordered phases and disordered phases, while DODSe SAMs formed in 1 mM and 5 mM solutions have only disordered phases with an abnormally high VI fraction of 22-24%. From STM, CV, and CA measurements, we also found that the wetting property and electrochemical behavior of DODSe SAMs is strongly influenced by the formation of ordered SAMs and VI density. The molecular-scale STM results obtained here will be very useful in understanding dialkyl diselenide SAMs, as well as for obtaining high-quality SAMs with a high structural order.

Acknowledgements. This work was supported by the Korea Foundation for International Cooperation of Science & Technology (KICOS) through a grant provided from the

Korean Ministry of Science & Technology (MOST), No. K20501000002-07-E0100-00210. This work was also partly supported by the Seoul R&BD Program (10919).

References

1. Nuzzo, R. G.; Dubois, L. H.; Allara, D. L. *J. Am. Chem. Soc.* **1990**, *112*, 558.
2. Ulman, A. *Chem. Rev.* **1996**, *96*, 1533.
3. Love, J. C.; Estroff, L. A.; Kriebel, J. K.; Nuzo, R. G.; Whitesides, G. M. *Chem. Rev.* **2005**, *105*, 1103.
4. Poirier, G. E.; Pylant, G. E. *Science* **1996**, *272*, 1145.
5. Noh, J.; Kato, H. S.; Kawai, M.; Hara, M. *J. Phys. Chem. B* **2006**, *110*, 2793.
6. Noh, J.; Jeong, Y.; Ito, E.; Hara, M. *J. Phys. Chem. C* **2007**, *111*, 2691.
7. Noh, J. *Bull. Korean Chem. Soc.* **2006**, *27*, 944.
8. Jeong, Y.; Han, J. W.; Kim, N.; Lee, Y.; Hara, M.; Noh, J. *Bull. Korean Chem. Soc.* **2007**, *28*, 2445.
9. Choi, Y.; Jeong, Y.; Chung, H.; Ito, E.; Hara, M.; Noh, J. *Langmuir* **2008**, *24*, 91.
10. Noh, J.; Hara, M. *Langmuir* **2002**, *18*, 1953.
11. Samant, M. G.; Brown, C. A.; Gordon, J. G. *Langmuir* **1992**, *8*, 1615.
12. Nakano, K.; Sato, T.; Tazaki, M.; Tagaki, M. *Langmuir* **2000**, *16*, 2225.
13. Dishner, M. H.; Hemminger, J. C.; Feher, F. J. *Langmuir* **1997**, *13*, 4788.
14. Huang, F. K.; Horton, R. C. Jr.; Myles, D. C.; Garrell, R. L. *Langmuir* **1998**, *14*, 4802.
15. Han, S. W.; Kim, K. *J. Colloid Interface Sci.* **2001**, *240*, 492.
16. Han, S. W.; Lee, S. J.; Kim, K. *Langmuir* **2001**, *17*, 6981.
17. Gladysz, J. A.; Homby, J. L.; Garbe, J. E. *J. Org. Chem.* **1978**, *43*, 1204.
18. Monnell, J. D.; Stapleton, J. J.; Jackiw, J. J.; Dunbar, T.; Reinert, T.; Dirk, S. M.; Tour, J. M.; Allara, D. L.; Weiss, P. S. *J. Phys. Chem. B* **2004**, *108*, 9834.
19. Shaporenko, A.; Ulman, A.; Terfort, A.; Zharnikov, M. *J. Phys. Chem. B* **2005**, *109*, 3898.
20. Shaporenko, A.; Cyganik, P.; Buck, M.; Ulman, A.; Zharnikov, M. *Langmuir* **2005**, *21*, 8204.
21. Noh, J.; Hara, M. *Langmuir* **2001**, *17*, 7280.
22. Lukkari, J.; Meretoja, M.; Kartio, L.; Laajalehto, K.; Rajamäki, M.; Linderstöm, M.; Kankare, J. *Langmuir* **1999**, *15*, 3529.
23. Peterlinz, K.; Georgiadis, R. *Langmuir* **1996**, *12*, 4731.